Human Apolipoprotein C-II Forms Twisted Amyloid Ribbons and Closed Loops†

Danny M. Hatters,‡ Cait E. MacPhee,§ Lynne J. Lawrence,|| William H. Sawyer,‡ and Geoffrey J. Howlett*,‡

Department of Biochemistry and Molecular Biology, The University of Melbourne, Parkville, Victoria 3052, Australia, Oxford Centre for Molecular Sciences, New Chemistry Laboratory, University of Oxford, South Parks Road, OX1 3QT, United Kingdom, and Biomolecular Research Institute, Parkville, Victoria 3052, Australia

Received January 4, 2000; Revised Manuscript Received March 9, 2000

ABSTRACT: Human apolipoprotein C-II (apoC-II) self-associates in solution to form aggregates with the characteristics of amyloid including red-green birefringence in the presence of Congo Red under cross-polarized light, increased fluorescence in the presence of thioflavin T, and a fibrous structure when examined by electron microscopy. ApoC-II was expressed and purified from *Escherichia coli* and rapidly exchanged from 5 M guanidine hydrochloride into 100 mM sodium phosphate, pH 7.4, to a final concentration of 0.3 mg/mL. This apoC-II was initially soluble, eluting as low molecular weight species in gel filtration experiments using Sephadex G-50. Circular dichroism (CD) spectroscopy indicated predominantly unordered structure. Upon incubation for 24 h, apoC-II self-associated into high molecular weight aggregates as indicated by elution in the void volume of a Sephadex G-50 column, by rapid sedimentation in an analytical ultracentrifuge, and by increased light scattering. CD spectroscopy indicated an increase in β-sheet content, while fluorescence emission spectroscopy of the single tryptophan revealed a blue shift and an increase in maximum intensity, suggesting repositioning of the tryptophan into a less polar environment. Electron microscopy of apoC-II aggregates revealed a novel looped-ribbon morphology (width 12 nm) and several isolated closed loops. Like all of the conserved plasma apolipoproteins, apoC-II contains amphipathic helical regions that account for the increase in α-helix content on lipid binding. The increase in β-structure accompanying apoC-II fibril formation points to an alternative folding pathway and an in vitro system to explore the general tendency of apolipoproteins to form amyloid in vivo.

Human apolipoprotein C-II (apoC-II)[1] is a conserved member of a family of plasma apolipoproteins that serve in the blood lipid transport system. Mature apoC-II, composed of 79 amino acids is found predominantly in chylomicrons and very low-density lipoproteins (VLDL) from which it is purified (*1*). ApoC-II activates lipoprotein lipase and in this capacity is an important regulator of blood triacylglycerol hydrolysis (*2*−*5*). Although previous work using purified apoC-II has indicated a slow aggregation (*6*−*8*), most attention has concentrated on the state of association of soluble, low molecular weight apoC-II. During the course of our work on the solution properties of apoC-II, we observed a time-dependent increase in the amount of β-structure, as revealed by circular dichroism (CD) spectroscopy and considered whether this may be due to amyloid formation.

Amyloid fibrils are unbranched rigid fibers of protein of indefinite length and between 7- and 18-nm wide (*9*, *10*). Proteins that form amyloid are diverse with no homology to each other although all form an ordered β-sheet interacting structure made up of protofilaments (typically 2.5−3.5 nm wide) that associate in bundles to form fibrils (*10*). Most cases of pathological amyloid deposits are believed to be due to either misfolded or mutant forms of native proteins (*9*, *11*). Amyloid fibrils of certain proteins have been linked to several prominent diseases including Alzheimer's disease with the Aβ peptide (*12*), type II diabetes with islet amyloid polypeptide (*13*, *14*), and Creutzfeldt−Jakob disease with the prion protein (*15*). Other proteins such as the SH3 domain of phosphatidylinositol-3′-kinase have been shown to form amyloid in vitro but not in vivo (*16*). A characteristic feature of amyloidogenic proteins is their small size with monomer molecular weights generally under 30 kDa (*9*).

A significant number of apolipoproteins, apoA-I (*17*), murine apoA-II (*18*), apoE (*19*), and serum amyloid A (*20*) have been implicated in amyloidogenic diseases or have been shown to form amyloid. Proteolytic 10 kDa N-terminal fragments of a rare isoform of apoA-I have been identified in amyloid fibrils isolated from the spleen of patients with autosomal dominant nonneuropathic systemic amyloidosis (*21*). An isoform of apoA-II in inbred mice was linked by restriction fragment length polymorphism to inherited senile amyloidosis (*18*) and was later identified in senile plaques (*22*). Amyloid A, consisting of two-thirds of the apolipoprotein serum amyloid A, has been identified in amyloid

† This work was funded by the National Health and Medical Research Council and the Australian Research Council.

* To whom correspondence should be addressed. Phone: +61 3 9344 7632. Fax: +61 3 9347 7730. E-mail: g.howlett@biochemistry.unimelb.edu.au.

‡ The University of Melbourne.

§ University of Oxford.

|| Biomolecular Research Institute.

[1] Abbreviations: apoC-II, apolipoprotein C-II; LpL, lipoprotein lipase; CD, circular dichroism; VLDL, very low-density lipoproteins; SDS−PAGE, sodium dodecyl sulfate−polyacrylamide gel electrophoresis; MBP, maltose binding protein; PCR, polymerase chain reaction; ThT, thioflavin T; FRET, fluorescence energy transfer; TFE, trifluroethanol.

10.1021/bi000002w CCC: $19.00
Published on Web 06/20/2000

deposits within the spleen, liver, and kidneys of a minority of patients with chronic inflammatory diseases (*20*). Of current research interest is the apoE4 isoform, which, while not forming amyloid itself, has been found in amyloid plaques of patients with Alzheimer's disease (*23*) and is believed to bind to and influence the formation of Aβ fibrils (*24*). The present work investigates the aggregation of apoC-II and characterizes the amyloid-like nature of the structures that are formed.

MATERIALS AND METHODS

Expression and Purification of apoC-II. A plasmid containing cDNA for human apoC-II (*25*) was kindly provided by Dr N. S. Shachter (Rockefeller University, NY). ApoC-II was expressed in *E. coli* using PCR-generated DNA cloned into the pET11a expression vector (Novagen) as described previously (*26*). The DNA sequence was confirmed by sequencing with the PRISM system (Perkin-Elmer). ApoC-II was expressed in 4 L of media (*26*). After inclusion bodies were washed, they were resuspended in 5 mL of 5 M guanidine HCl, and 100 mM arginine, pH 12.0. The solution was sonicated for 1 min on medium power with a medium probe (Soniprep 150, MSE Scientific Instruments), and the remaining insoluble material was removed by centrifugation at 15000*g* for 5 min at room temperature. The solution was diluted to 40 mL with 5 M guanidine HCl and applied, in 500-μL aliquots, to a HR10-30 column (Pharmacia-Biotech) packed with Superdex 75 gel filtration resin (Pharmacia-Biotech) equilibrated in 6 M urea and 10 mM Tris-HCl, pH 8.0. Two peaks eluted from the column, and the second peak (at 10−14 mL), containing apoC-II, was collected. The apoC-II fractions were applied to a 2.5 × 6 cm column packed with DEAE-Sephacel anion-exchange resin (Pharmacia-Biotech) equilibrated in 6 M urea and 10 mM Tris-HCl, pH 8.0, at 2 mL/min. The apoC-II was eluted using a 0−500 mM NaCl gradient in the above buffer over 250 mL at a flow rate of 3 mL/min. The apoC-II eluted at approximately 120 mM NaCl. The eluted apoC-II was exhaustively dialyzed against 10 mM NH_4HCO_3, pH 8.0, at 4 °C. The apoC-II was lyophilized and stored as a stock in 5 M guanidine HCl at −20 °C. The purity of the apoC-II was similar to that previously described (*26*) (>95%) as estimated by Coomassie Brilliant Blue R250 staining on Tris-tricine SDS−PAGE (*27*). Matrix-assisted laser desorption ionization time-of-flight mass spectrometry internally calibrated with human insulin and horse heart cytochrome C revealed that approximately 65% of the apoC-II had a molecular weight equivalent to that of native apoC-II (molecular weight = 8915), while the molecular weight of the remainder was consistent with an extra N-terminal methionine (molecular weight = 9046), as observed previously (*26*). The concentration of the apoC-II was determined using an extinction coefficient of 12 090 M^{-1} cm^{-1} in denaturant (*28*) and 12 950 M^{-1} cm^{-1} when refolded (*29*). Typical yields were approximately 60 mg of pure apoC-II/4 L of culture.

ApoC-II was also expressed as a fusion with maltose binding protein using the pMAL-c2 expression vector (New England Biolabs). The concentration of MBP-apoC-II was determined by measuring the absorbance at 280 nm using an extinction coefficient of 79 300 M^{-1} cm^{-1} (*29*). The fusion protein was proteolytically cleaved (16 h at room temperature) with factor Xa (Pharmacia-Biotech) to release apoC-II from MBP using a ratio of 1 unit factor Xa to 150 μg fusion protein. The cleaved products were purified by gel filtration using a Superdex 75 preparative resin (Pharmacia-Biotech) equilibrated in 4 M guanidine HCl and 20 mM sodium phosphate, pH 7.4. Tris-tricine SDS−PAGE (*27*) confirmed that the purity was above 95% as visualized with Coomassie brilliant blue R250, and electrospray mass spectrometry indicated that the molecular weight of the product was equal to that predicted for native apoC-II (8915). Unless indicated, experiments were performed with apoC-II derived from the pET11a expression system.

Refolding of apoC−II. As misfolding induces aggregation of recombinant proteins (*30*), we chose to refold apoC-II at a relatively low concentration and add 100 mM urea to the buffers after the protein was refolded to inhibit intermolecular hydrophobic interactions. A stock of apoC-II at 9.5 mg/mL in 5 M guanidine HCl was diluted directly into 100 mL of 100 mM sodium phosphate, pH 7.4, to a final protein concentration of 50 μg/mL. The protein was incubated at room temperature for 3 h and then dialyzed into 100 mM urea and 10 mM sodium phosphate, pH 7.4, at 4 °C with two buffer changes. The protein solution was applied to a HR5-10 column (Pharmacia-Biotech) packed with Source 15Q anion-exchange resin (Pharmacia-Biotech) preequilibrated in 100 mM urea, 10 mM sodium phosphate, pH 7.4. The protein was eluted with the above buffer and 500 mM NaCl at a flow rate of 1 mL/min. The eluted protein was desalted by application to a 1 × 9 cm column of Sephadex G-25 resin preequilibrated with 100 mM sodium phosphate, pH 7.4, and eluted at a flow rate of 1 mL/min. ApoC-II prepared by this method and used directly is referred to as freshly prepared.

CD Measurements. CD spectra were recorded in a model 62DS AVIV CD spectrometer. The spectra were measured in 1-mm quartz cuvettes, and data were collected from 250 to 195 nm at 0.5-nm intervals. The samples were all in 100 mM sodium phosphate, pH 7.4. The bandwidth was set at 1.5 nm, and the temperature was set at 20 °C. The mean residue ellipticity, [θ], was calculated from the equation [θ] = θ/(*cnl*/M) where *l* is path length in mm, θ is observed ellipticity in millidegrees, *c* is concentration of protein (mg/mL), *n* is number of amino acid residues, and *M* is the molecular weight. Spectra were corrected for baseline using the spectrum for buffer alone.

Analytical Gel Filtration of Refolded apoC-II. An HR10-30 column (Pharmacia-Biotech) was packed with Sephadex G-50 and equilibrated in 100 mM sodium phosphate, pH 7.4. Samples were loaded in 200-μL aliquots and eluted at a flow rate of 0.5 mL/min. The eluent was monitored by absorption at 280 nm. A calibration curve was constructed using the following: aprotinin (molecular weight = 6511), cytochrome C (12 400), ribonuclease A (13 700), myoglobin (17 200), α-chymotrypsinogen A (25 000), and bovine serum albumin (67 000).

Analytical Ultracentrifugation. Samples were analyzed by analytical ultracentrifugation (XL-A analytical ultracentrifuge, Beckman/Coulter) using a double sector filled Epon centerpiece. Radial optical densities were measured at 280 or 230 nm. Sedimentation coefficients were determined either by direct numerical fitting of the sedimentation profiles (*31*) or by estimating from plots of $\omega^2 t$ versus the natural log of the radius of the midpoint of the sedimenting boundary. The

partial specific volume of apoC-II was estimated from the amino acid composition (*32*).

Light Scattering Measurements. The absorption of the samples at 350 nm was monitored over 45 h in a Cary-5 spectrophotometer (Varian) in 1-cm quartz cuvettes at 20 °C. The samples were sealed with Nescofilm to prevent evaporation. Buffer alone was included as a baseline reference, and the samples were not stirred during the assay.

Fluorescence Measurements of the Single Tryptophan in apoC-II. The emission spectrum of apoC-II was collected with the excitation wavelength at 295 nm in a Perkin-Elmer LS-5 luminescence spectrometer with excitation and emission slit widths of 2.0 nm.

Thioflavin T Binding Assay. Samples (410 μL) contained 12.85 μg of protein, 24 μg of thioflavin T (ThT), and 100 mM potassium phosphate, pH 7.0. The fluorescence measurements were recorded at 55° polarization in a SPEX fluorolog-τ2 spectrometer with the excitation and emission slit widths of 7.54 nm, in 0.5-cm quartz cuvettes. Excitation spectra were recorded with the emission wavelength set at 482 nm. Emission spectra were recorded with the excitation wavelength set at 450 nm. The protein contributions to the fluorescence spectra were minimal and were subtracted from the spectra.

Congo Red Binding Assay. A 500-μL solution of 2.5 μM Congo Red and 110 μg of apoC-II was prepared in 100 mM potassium phosphate, pH 7.4. The samples were incubated at room temperature for 5 min before measuring the absorbance spectra in 1-cm quartz cuvettes in a Cary-5 spectrophotometer (Varian). Any protein absorbance contributions were subtracted from the spectra and are not shown.

Light Microscopy. A 3-mL solution of apoC-II in 100 mM sodium phosphate, pH 7.4 ($\sim$0.3 mg/mL), left to aggregate over 1 day was concentrated using a centricon YM-3 ultrafiltration membrane (Amicon) until large gelatinous clumps were visible ($\sim$100 μL). The aggregate was stained with Congo Red to a final concentration of 1.7 mM Congo Red from a 10 mM stock. After 1 h, the aggregate was collected by brief centrifugation at 15000*g*, resuspended in 80 μL of water, spread on a glass microscope slide, and covered with a coverslip. Excess Congo Red was removed with water. The samples were viewed under bright-field and cross-polarized light in a Leica Wild Heerburg M3Z microscope, and the images were recorded with a Canon EOS100 camera.

Transmission Electron Microscopy. Copper grids (400 mesh) were coated with thin carbon film and glow discharged in nitrogen. Samples of apoC-II (0.1−0.3 mg/mL) were applied to the grids for 1 min within 15 min of glow discharging and then washed with water followed by stain, in the case of uranyl acetate or uranyl formate, or washed immediately with several drops of stain, in the case of potassium phosphotungstate or methylamine tungstate. Grids were air-dried for up to an hour at room temperature and examined using a JEOL 2000FX TEM operating at 120 kV. Micrographs were recorded at nominal magnifications of $\times$100k and $\times$80k, and the microscope was calibrated by photographing tobacco mosaic virus under the same conditions (*33*). Micrographs were digitized for measurement on a Perkin-Elmer PDS 1010G microdensitometer using a 20-μm step.

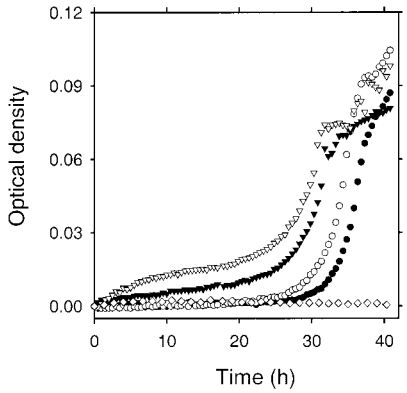

FIGURE 1: Light scattering measurements of freshly prepared apoC-II. Aggregation was monitored by light scattering at 350 nm. Samples were incubated at 20 °C with no stirring. Concentrations of apoC-II are 0.58 mg/mL (▽), 0.29 mg/mL (▼), 0.15 mg/mL (○), and 0.073 mg/mL (●). A scattering control was also performed using 0.25 mg/mL glycogen (◇).

RESULTS

Light Scattering Measurements. ApoC-II aggregation was initially monitored by light scattering at 350 nm (Figure 1). At lower concentrations of apoC-II (0.075 and 0.15 mg/mL), there was an initial lag phase with very little change in light scattering over a period of approximately 24 h followed by a more rapid increase over the next 16 h. At higher initial concentrations of apoC-II (0.3 and 0.6 mg/mL), there was an immediate slow increase in light scattering followed by a more rapid rise after approximately 24 h. Control experiments using 0.25 mg/mL glycogen showed no increase in light scattering over the time course. The results with apoC-II indicate a lag phase followed by a rapid aggregation phase. This kinetic behavior is similar to that of amyloid formation reported in other systems (*34*, *35*).

Gel Filtration Analysis. The state of association of apoC-II was further investigated by analytical gel filtration. Freshly prepared apoC-II was soluble (0.3 mg/mL) as demonstrated by gel filtration on Sephadex G-50. Comparison of the elution volume obtained with values determined for standard proteins indicated an average molecular weight (19 000) corresponding to apoC-II dimer. Only a small proportion of this freshly refolded apoC-II eluted at the void volume (approximately 5%). In contrast, an aliquot of the same solution of apoC-II after 16 h incubation at room temperature eluted predominantly at the void volume of the column, suggesting that most of the apoC-II had aggregated into larger oligomers.

Sedimentation Velocity Analysis of apoC-II. Freshly prepared apoC-II after 1 h incubation was analyzed by sedimentation velocity experiments in an analytical ultracentrifuge. Initial scans taken at 4-min intervals showed a fast moving boundary corresponding to approximately 20% of the total optical density (Figure 2A). Subsequent scans taken at 12-min intervals indicated that the majority of apoC-II under these conditions migrated as a slower moving boundary (Figure 2A). Analysis of the time dependence of this slower boundary (*31*) gave good fits of the data to a single sedimenting species of molecular weight 10 000 and a sedimentation coefficient of 1S. This suggests that the majority of freshly prepared apoC-II is composed of monomers. This result is in contrast to the results suggested by

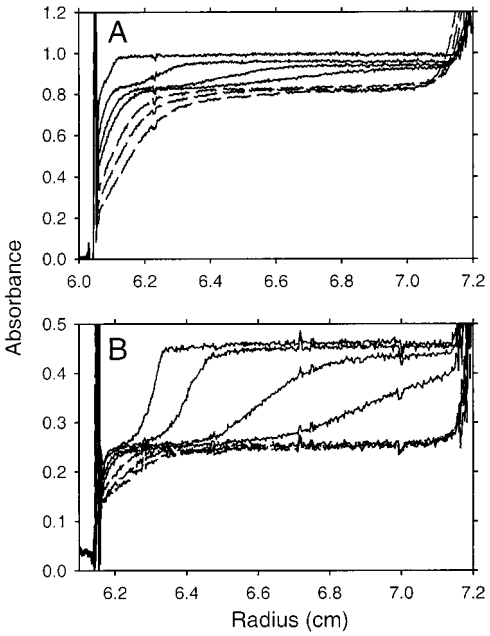

FIGURE 2: Sedimentation velocity profiles of apoC-II at 50 000 rpm in an analytical ultracentrifuge (XL-A) at 20 °C. Solid lines indicate first four radial scans taken at 4-min intervals. Dashed lines indicate three further scans taken at 12-min intervals. (A) Freshly prepared apoC-II (OD at 230 nm). (B) ApoC-II after incubation for 3 days at room temperature (OD at 280 nm).

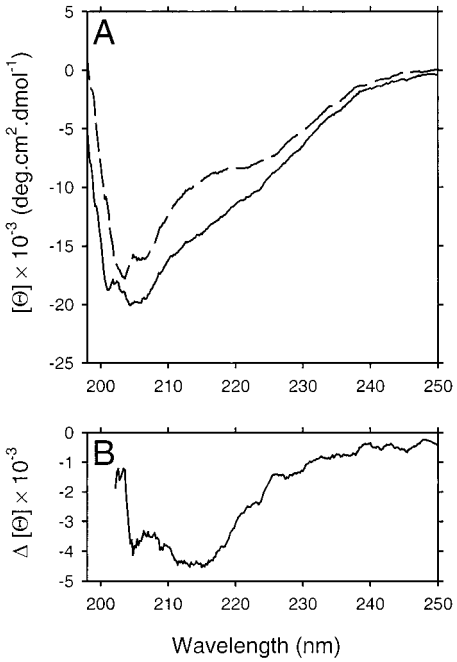

FIGURE 3: Circular dichroism spectra of freshly prepared and 1-day incubated apoC-II at 0.3 mg/mL. (A) Spectra were recorded of freshly prepared apoC-II (dashed line) and of apoC-II after a further 16-h incubation at room temperature (solid line). (B) Difference spectrum of freshly prepared and 1-day incubated apoC-II.

the gel filtration experiments. Possible explanations for the discrepancy are that the gel filtration results are affected by the presence of the faster migrating species or that lipid-free apoC-II is asymmetric and does not elute from the column according to the molecular weight of the standard proteins used to calibrate the column (*8*). The important conclusion is that freshly prepared apoC-II consists mainly of low molecular weight species.

The sedimentation profile of apoC-II incubated for 3 days is shown in Figure 2B. The striking observation is that approximately 50% of the optical density in the initial boundary sediments rapidly. The capacity of apoC-II to aggregate has been observed in previous work on the solution properties of apoC-II (*6*−*8*). Attempts were made to analyze the data in Figure 2B assuming two sedimenting species in which the molecular weight and sedimentation coefficient of the slower species were constrained to the values obtained from the analysis of Figure 2A. These results were unsuccessful due to extensive spreading of the faster boundary, presumably as the result of significant molecular heterogeneity. Consideration of the rate of movement of the midpoint of the fast boundary yielded an estimate of the average sedimentation coefficient of 65S. A separate sample of 1-day incubated apoC-II was analyzed by centrifugation at a lower angular velocity (5000 rpm) yielding an estimate of 84S for the average sedimentation coefficient. An estimate for the average molecular weight of the aggregate can be made by assuming a spherical shape and a normal partial specific volume (0.73 mL/g) and level of hydration (0.4 g/g of protein). For this case, a sedimentation coefficient of 80S corresponds to a spherical protein of molecular weight 3.5×10^6 implying that the apoC-II aggregate is composed of at least 400 subunits. This calculation represents a lower limit of the degree of aggregation since, as indicated below, the apoC-II aggregate has a fibrous morphology.

Circular Dichroism of apoC-II. A CD spectrum of freshly prepared apoC-II is shown in Figure 3A. The secondary structure was consistent with predominantly unordered structure with a characteristic minimum at 202 nm, similar to that previously reported (*8*). The slight shoulder at approximately 222 nm suggests a small amount of residual α-helix. A previously published CD spectrum of apoC-II by Mantulin et al. (*7*) indicates a content of approximately 30% α-helix and 18% *β*-sheet. ApoC-II incubated for 1 day exhibited increased negative ellipticities as compared to the spectrum of freshly prepared apoC-II (Figure 3A). Analysis of the difference spectrum (Figure 3B) revealed a maximum change at 215 nm. This change suggests an increase in *β*-sheet structure at the expense of unordered and helical structure and is characteristic of the changes in secondary structure that accompany amyloid formation (*10*).

Tryptophan Emission Spectrum. Incubation of apoC-II leads to changes in the fluorescence of the single tryptophan at position 26 of the mature native protein. The emission spectrum of freshly prepared apoC-II shows a maximum at 342 nm with excitation at 295 nm (Figure 4). After incubation for 1 day, the fluorescence intensity increases 35%, and the wavelength of maximum emission is blue-shifted to 335 nm. The shift in the wavelength of maximum emission to a lower wavelength indicates a transition of the tryptophan residue to a more hydrophobic environment, reflecting either the time-dependent change in secondary structure (Figure 3) or the consequences of apoC-II aggregation.

Thioflavin T Binding. A characteristic of amyloid deposits is the capacity to bind to ThT, an event that can be detected using fluorescence spectroscopy (*36*). Addition of ThT to freshly prepared apoC-II resulted in a 2-fold increase in the excitation intensity at 430 nm of ThT and a new excitation peak at 280 nm (Figure 5A). The addition of ThT to apoC-

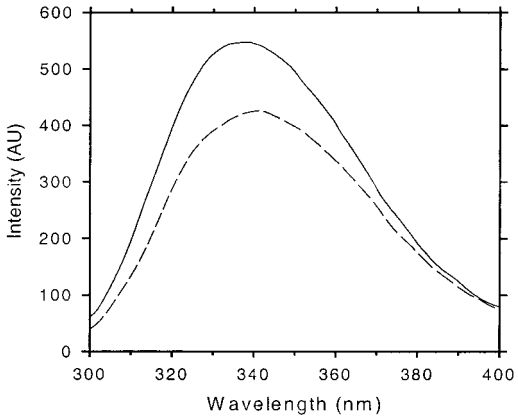

FIGURE 4: Emission spectrum of the single tryptophan in apoC-II. Spectra were recorded with the excitation wavelength set at 295 nm of freshly prepared apoC-II (dashed line) and of apoC-II after 1-day incubation at room temperature (solid line).

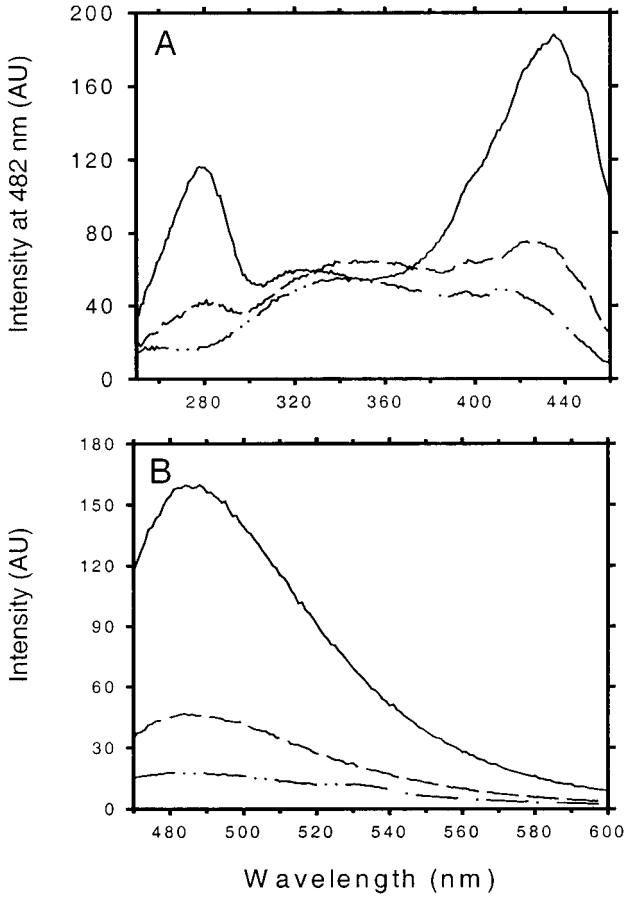

FIGURE 5: Fluorescence spectrum of thioflavin T in the presence and absence of freshly prepared or incubated apoC-II. (A) Excitation spectrum of ThT was recorded with emission intensity collected at 482 nm in the absence of protein (dashed−dotted line), in the presence of freshly prepared apoC-II (dashed line), and in the presence of apoC-II that was incubated for 1 day after fresh preparation (solid line). (B) Emission spectrum of ThT was recorded with the excitation wavelength 450 nm in the absence of protein (dashed−dotted line), in the presence of freshly prepared apoC-II (dashed line), and in the presence of 1-day incubated apoC-II (solid line). Scattering contributions of the protein were subtracted from the spectra.

II after 1-day incubation resulted in a 5-fold increase in the excitation peak at 430 nm as compared to ThT alone and a substantial increase in the peak at 280 nm (Figure 5A). The

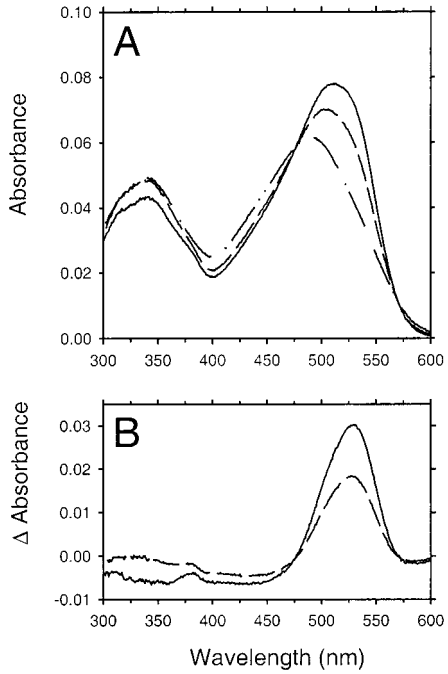

FIGURE 6: (A) Absorption spectrum of Congo Red in the presence and absence of freshly prepared apoC-II or 1-day incubated apoC-II. Spectra shown are Congo Red alone at 2.5 μM (dashed−dotted line), Congo Red with 110 μg of freshly prepared apoC-II (dashed line), and Congo Red with 110 μg of apoC-II that was incubated for 1 day after fresh preparation (solid line). (B) Difference spectrum of Congo Red in the presence of apoC-II (freshly prepared, dashed line and 1-day incubated apoC-II, solid line) relative to Congo Red alone. Scattering contributions of the protein were subtracted from the spectra.

strong excitation peak centered on 280 nm in the excitation spectrum is an interesting observation and can be explained by fluorescence resonance energy transfer (FRET) between the single tryptophan residue in apoC-II and the bound ThT. This provides additional evidence for close association between ThT and aggregated apoC-II. This effect is not observed with the aggregated Aβ peptide that lacks tryptophan (*36*).

Changes were also observed in the emission spectra of ThT. When the emission spectrum of ThT was recorded in the presence of freshly prepared apoC-II, there was a 2-fold increase in the emission at 482 nm upon excitation at 450 nm as compared to ThT alone (Figure 5B). In the presence of 1-day incubated apoC-II, there was an 8-fold increase in emission of ThT at 482 nm (Figure 5B). These changes in ThT fluorescence are consistent with apoC-II having amyloid structure when aggregated and, apart from the new excitation peak at 280 nm, are very similar to that observed for Aβ amyloid (*36*).

Congo Red Binding. We further investigated the amyloid-like properties of the apoC-II aggregate by measuring the binding to another amyloid dye, Congo Red. Congo Red alone has an absorbance maximum at a wavelength of 490 nm (Figure 6A). When freshly prepared apoC-II was added to Congo Red, the maximum absorbance red-shifted to 510 nm, and the absorbance increased 15% (Figure 6A). The addition of an equivalent amount of 1-day incubated apoC-II to Congo Red resulted in a further increase in the absorbance maximum to approximately 515 nm and a 13% increase in the absorbance (Figure 6). The difference

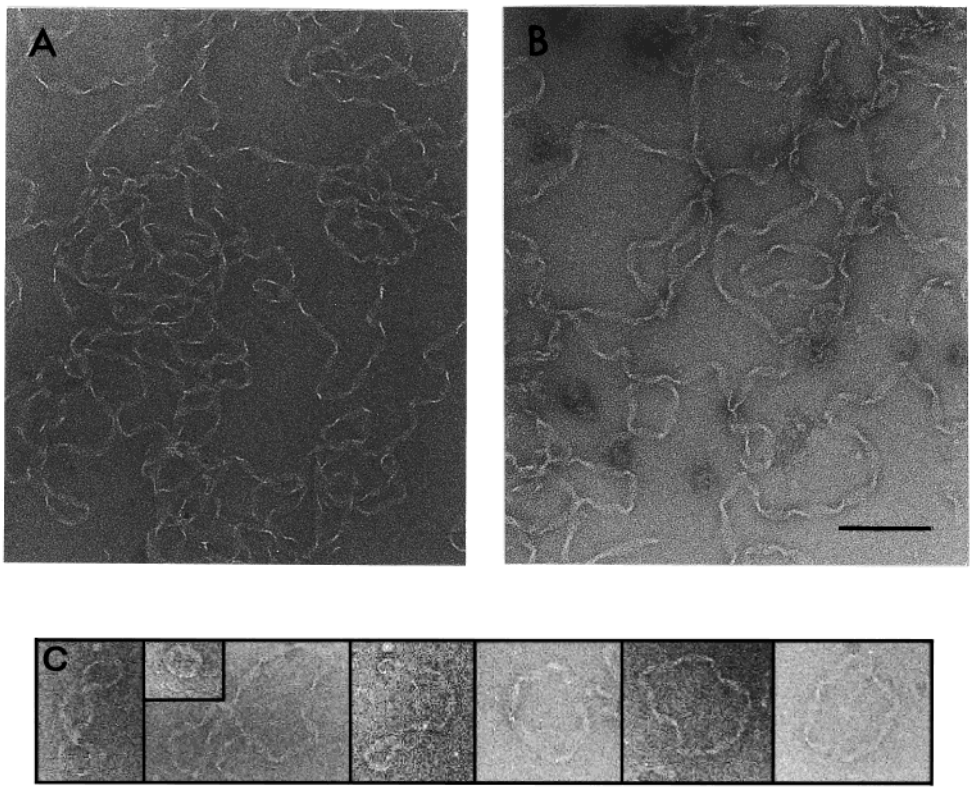

FIGURE 7: ApoC-II fibrils imaged by transmission electron microscopy. ApoC-II fibrils were formed by incubation of apoC-II at 300 μg/mL in 100 mM sodium phosphate, pH 7.4, for 2 days. (A) ApoC-II stained with potassium phosphotungstate. Note the flat ribbonlike morphology. (B) ApoC-II stained with uranyl formate. The semiregular helical structure is more apparent when potassium phosphotungstate is used. (C) Montage of closed loop structures obtained under a range of staining conditions. Scale bar 100 nm.

spectrum (Figure 6B) revealed a maximum change in the absorption at 530 nm, similar to Aβ amyloid (*37*).

An essential feature of Congo Red bound to amyloid structures is red-green birefringence under cross-polarized light. When apoC-II aggregates were bound to Congo Red, washed, and viewed under bright field microscope, they were clearly visible as red, gelatinous aggregates. Under cross-polarized light, these aggregates were strongly apple-green birefringent, a hallmark characteristic of amyloid structure (*38*).

Transmission Electron Microscopy. ApoC-II was incubated for 16 h and examined by electron microscopy. The results in Figure 7 reveal fibrous structures of indeterminate length due to tangled nature of the fibrils. The looped ribbon morphology in Figure 7 has an approximate width of 12 nm and a helical repeat of approximately 27 nm with a range of 20−35 nm. This repeat distance may be compared to published results for other amyloid fibrils of 11.5 nm (*39*), 20 nm (*40*), and 50−60 nm (*41*). A number of looped structures were also observed with selected examples included as a montage in Figure 7. These loops were typically 50−75 nm in diameter and appear to be continuous and not simply overlapping linear fibrils. Repeated preparations of apoC-II at pH 7.4 and preparations of apoC-II aggregate at pH values of 6, 8, and 10 revealed similar looped ribbon morphology and the presence of isolated loops, as did samples incubated for up to 1 month.

DISCUSSION

Many of the proteins previously identified with amyloid deposits in vivo either contain mutations or, as in the case of the βA4 peptide, are processed via alternative cleavage pathways (*42*). We therefore considered whether our observation of amyloid formation by recombinant apoC-II may be due to the addition of an unnatural N-terminal methionine in 35% of the apoC-II expressed from the pET11a expression vector. To test this hypothesis, we utilized a hybrid fusion protein obtained using the pMAL-c2 expression vector to express and purify native apoC-II lacking the additional N-terminal methionine. This protein demonstrated the same aggregation properties as that produced from the pET11a expression system, as indicated by light scattering studies, ThT binding, and sedimentation analysis using the analytical ultracentrifuge. Aggregation of apoC-II isolated from plasma (*6*−*8*) provides supporting evidence that amyloid formation is not driven by the N-terminal methionine of pET11a derived apoC-II.

Insight into the mechanism of amyloid formation by proteins is provided by recent studies of naturally occurring variants of human lysozyme (*43*). These studies show that mutant forms of lysozyme that generate amyloid also exhibit many factors characteristic of the molten globular state. Lysozymes containing Ile56Thr or Asp67His mutations binds ANS, exchange protons rapidly within internal domains, denature readily, and have full secondary structure as demonstrated by CD spectroscopy. Similar observations have also been observed for mutant forms of transthyretin (*44*), leading to the conclusion that amyloid formation occurs via the self-association of compact folding intermediates (*45*).

Apolipoproteins also have properties characteristic of the molten globular state. Thermal denaturation of lipid-free apoA-I suggests stable α-helical secondary structure but

loosely defined tertiary structure at near physiological conditions (*46*). Monomeric apoC-I has some of the properties of loosely folded tertiary structure in the absence of lipid (*47*), while apolipophorin III binding to lipid correlates with an increased hydration of the protein interior suggesting lipid binding occurs via the formation of a molten globular state (*48*). On this basis, we postulate that lipid-free apoC-II exists as a compact but flexible intermediate in solution with lipid binding and amyloidosis presenting as alternative pathways. Support for this hypothesis is provided by our light scattering experiments (results not shown) demonstrating inhibition of apoC-II aggregation by micellar concentrations of dihexanoylphosphatidylcholine (16 mM). Under these conditions, apoC-II acquires significant α-helical structure as demonstrated by CD spectroscopy (results not shown). While these experiments suggest lipid binding predominates over amyloid formation under normal conditions, free pools of exchangeable apolipoproteins exist in plasma (*49*) such that mutations or proteolysis events that destabilize lipid binding could accentuate the propensity of this free pool to form amyloid in vivo.

In common with other apolipoproteins, apoC-II contains extensive amphipathic α-helical sequences postulated to mediate the binding to lipid surfaces (*50*) and to account for the increase α-helical content on lipid binding. The results in Figure 3 indicate an increase in β-structure on amyloid formation by apoC-II at the expense of unordered and helical structure. While the exact region of apoC-II involved in amyloid conformation is not known, one possibility is that the amphipathic helical region(s) of apoC-II undergo an α-helix to β-sheet transition, characteristic of the pathway of amyloid formation in other systems (*51*, *52*). Support for this idea comes from our previous studies with peptides derived from apoC-II (*53*). An amphipathic peptide derivative of apoC-II (apoC-II_{19-39}) undergoes significant structural changes in the presence of trifluoroethanol (TFE). At a TFE concentration of approximately 30%, apoC-II_{19-39} acquires significant α-helical structure. However, higher concentrations of TFE (50−60%) promote further changes in apoC-II_{19-39}, generating β-structure with the formation of material that sediments rapidly in the analytical ultracentrifuge. This effect is not observed for the peptide apoC-II_{39-62}, in which TFE stabilizes helical structure but does not induce β-structure. TFE-mediated structural transitions between α-helix and β-sheet have also been reported for other amyloidogenic systems (*54*). The observation that the amphipathic helical region present in apoC-II_{19-39} can adopt a β-structure suggests a general mechanism where the amphipathic helical regions of apolipoproteins drive amyloid formation, an event that may explain the general prevalence of apolipoproteins in amyloid-related diseases.

ACKNOWLEDGMENT

We would like to thank Jocelyn Carpenter, at the School of Botany, University of Melbourne, for her assistance with electron microscopy. We also thank Bostjan Kobe and Ken Mitchellhill, at St. Vincent's Institute of Medical Research, 41 Victoria Parade, Fitzroy, Victoria, for help with the light microscopy and electrospray mass spectrometry.

REFERENCES

1. Jackson, R. L., and Holdsworth, G. (1986) *Methods Enzymol. 128*, 288−297.
2. LaRosa, J. C., Levy, R. I., Herbert, R., Lux, S. E., and Fredrickson, D. S. (1970) *Biochem. Biophys. Res. Commun. 41*, 57−62.
3. Havel, R. J., Fielding, C. J., Olivecrona, T., Shore, V. G., Fielding, P. E., and Egelrud, T. (1973) *Biochemistry 12*, 1828−1833.
4. Kinnunen, P. K., Jackson, R. L., Smith, L. C., Gotto, A. M., Jr., and Sparrow, J. T. (1977) *Proc. Natl. Acad. Sci. U.S.A. 74*, 4848−4851.
5. Fojo, S. S., and Brewer, H. B. (1992) *J. Intern. Med. 231*, 669−677.
6. Brown, W. V., Levy, R. I., and Fredrickson, D. S. (1970) *J. Biol. Chem. 245*, 6588−6594.
7. Mantulin, W. W., Rohde, M. F., Gotto, A. M., Jr., and Pownall, H. J. (1980) *J. Biol. Chem. 17*, 8185−8191.
8. Tajima, S., Yokoyama, S., Kawai, Y., and Yamamoto, A. (1982) *J. Biochem. 91*, 1273−1279.
9. Sipe, J. D. (1992) *Annu. Rev. Biochem. 61*, 947−975.
10. Sunde, M., and Blake, C. (1997) *Adv. Protein Chem. 50*, 123−159.
11. Kelly, J. W. (1996) *Curr. Opin. Struct. Biol. 6*, 11−17.
12. Masters, C. L., Simms, G., Weinman, N. A., Multhaup, G., McDonald, B. L., and Beyreuther, K. (1985) *Proc. Natl. Acad. U.S.A. 82*, 4245−4249.
13. Westermark, P., and Wilander, E., (1978) *Diabetologia 15*, 417−421.
14. Westermark, P., Wilander, E., Westermark, G. T., and Johnson, K. H. (1987) *Diabetologia 30*, 887−892.
15. Prusiner, S. B. (1998) *Proc. Natl. Acad. Sci. U.S.A. 95*, 13363−13383.
16. Guijarro, J. I., Sunde, M., Jones, J. A., Campbell, I. D., and Dobson, C. M. (1998) *Proc. Natl. Acad. Sci. U.S.A. 95*, 4224−4228.
17. Genschel, J., Haas, R., Propsting, M. J., and Schmidt, N. H. (1998) *FEBS Lett. 430*, 145−149.
18. Higuchi, K., Kitagawa, K., Naiki, H., Hanada, K., Hosokawa, M., and Takeda, T. (1991) *Biochem. J. 279*, 427−433.
19. Strittmatter, W. J., and Roses, A. D. (1995) *Proc. Natl. Acad. Sci. U.S.A. 92*, 4725−4727.
20. Levin, M., Pras, M., and Franklin, E. C. (1973) *J. Exp. Med. 138*, 373−380.
21. Soutar, A. K., Hawkins, P. N., Vigushin, D. M., Tennent, G. A., Booth, S. E., Hutton, T., Nguyen, O., Totty, N. F., Feest, T. G., Hsuan, J. J., et al. (1992) *Proc. Natl. Acad. Sci. U.S.A. 89*, 7389−7393.
22. Higuchi, K., Kogishi, K., Wang, J., Xia, C., Chiba, T., Matsushita, T., and Hosokawa, M. (1997) *Biochem. J.* 325, 653−659.
23. Strittmatter, W. J., and Roses, A. D. (1996) *Annu. Rev. Neurosci. 19*, 53−77.
24. Goedert, M., Strittmatter, W. J., and Roses, A. D. (1994) *Nature 372*, 45−46.
25. Jackson, C. L., Bruns, G. A. P., and Breslow, J. L. (1984) *Proc. Natl. Acad. Sci. U.S.A. 81*, 2945−2949.
26. Wang, C. S., Downs, D., Dashti, A., and Jackson K. W. (1996) *Biochim. Biophys. Acta 1302*, 224−230.
27. Schagger, H., and von Jagow, G. (1987) *Anal. Biochem. 166*, 368−379.
28. Edelhoch, H. (1967) *Biochemistry 6*, 1948−1954.
29. Pace, C. N., Vajdos, F., Fee, L., Grimsley, G., and Gray, T. (1995) *Protein Sci. 4*, 2411−2423.
30. De Bernardez Clark, E., Schwarz, E., and Rudolph, R. (1999) *Methods Enzymol. 309*, 217−236.
31. Schuck, P., MacPhee, C. E., and Howlett, G. J. (1998) *Biophys. J. 74*, 466−474.
32. Perkins, S. J. (1986) *Eur. J. Biochem. 157*, 169−180.
33. Mandelkow, E., and Holmes, K. C. (1974) *J. Mol. Biol. 87*, 265−273.
34. Jarret, J. T., and Lansbury, P. T., Jr. (1993) *Cell 73*, 1055−1058.

35. Evans, K. C., Berger, E. P., Cho, C.-G., Weisgraber, K. H., and Lansbury, P. T., Jr. (1995) *Proc. Natl. Acad. Sci. U.S.A. 92*, 763−767.
36. LeVine, H. (1993) *Protein Sci. 2*, 404−410.
37. Klunk, W. E., Jacob, R. F., and Mason, R. P. (1999) *Anal. Biochem. 266*, 66−76.
38. Divry, P., and Florkin, M. (1927) Sur les proprieties optiques de l′amyloid. *CR Soc. Biol. 97*, 1808−1810.
39. Crowther, R. A., Olesen, O. F., Smith, M. J., Jakes, R., and Goedert, M. (1994) *FEBS Lett. 337*, 135−138.
40. Jimenez, J. L., Guijarro, J. I., Orlova, E., Zurdo, J., Dobson, C. M., Sunde, M., and Saibil, H. R. (1999) *EMBO J. 18*, 815−821.
41. Sunde, M., Serpell, L. C., Bartlam, M., Fraser, P. E., Pepys, M. B., and Blake, C. C. (1997) *J. Mol. Biol. 273*, 729−739.
42. Sinha, S., and Lieberburg, I. (1999) *Proc. Natl. Acad. Sci. U.S.A. 96*, 11049−11053.
43. Booth, D. R., Sunde, M., Bellotti, V., Robinson, C. V., Hutchinson, W. L., Fraser, P. E., Hawkins, P. N., Dobson, C. M., Radford, S. E., Blake, C. C. F., and Pepys, M. (1997) *Nature 385*, 787−793.
44. Nettleton, E. J., Sunde, M., Lai, Z., Kelly, J. W., Dobson, C. M., and Robinson, C. V. (1998) *J. Mol. Biol. 281*, 553−564.
45. Dobson, C. M. (1999) *Trends Biochem. Sci. 24*, 329−332.
46. Gursky, O., and Atkinson, D. (1996) *Proc. Natl. Acad. Sci. U.S.A. 93*, 2991−2995.
47. Gursky, O., and Atkinson, D. (1998) *Biochemistry 37*, 1283−1291.
48. Soulages, J. L., and Bendavid, O. J. (1998) *Biochemistry 37*, 10203−10210.
49. Eisenberg S. (1984) *J. Lipid Res. 25*, 1017−1058.
50. Segrest, J. P., Jones, M. K., De Loof, H., Brouillette, C. G., Venkatachalapathi, Y. V., and Anantharamaiah, G. M. (1992) *J. Lipid Res. 33*, 141−166.
51. Nguyen, J., Baldwin, M. A., Cohen, F. E., and Prusiner, S. B. (1995) *Biochemistry 34*, 4186−4192.
52. Zhang, S., and Rich, A. (1997) *Proc. Natl. Acad. Sci. U.S.A. 94*, 23−28.
53. MacPhee, C. E., Perugini, M. A., Sawyer, W. H., and Howlett, G. J. (1997) *FEBS Lett. 416*, 265−268.
54. Chiti, F., Webster, P., Taddei, N., Clark, A., Stefani, M., Ramponi, G., and Dobson, C. M. (1999) *Proc. Natl. Acad. Sci. U.S.A. 96*, 3590−3594.

BI000002W